

Article

Protein Networks Associated with Native Metabotropic Glutamate 1 Receptors (mGlu₁) in the Mouse Cerebellum

Mahnaz Mansouri¹, Leopold Kremser², Thanh-Phuong Nguyen³, Yu Kasugai¹, Laura Caberlotto^{4,†}, Martin Gassmann⁵, Bettina Sarg², Herbert Lindner² , Bernhard Bettler⁵ , Lucia Carboni⁶  and Francesco Ferraguti^{1,*} 

¹ Department of Pharmacology, Medical University of Innsbruck, 6020 Innsbruck, Austria; mahnaz.mansouri@gmail.com (M.M.); kasugaiyu@yahoo.co.jp (Y.K.)

² Institute of Medical Biochemistry, Protein Core Facility, Medical University of Innsbruck, 6020 Innsbruck, Austria; leopold.kremser@i-med.ac.at (L.K.); bettina.sarg@i-med.ac.at (B.S.); herbert.lindner@i-med.ac.at (H.L.)

³ Dennemeyer, 1274 Hesperange, Luxembourg; nguyentp.dr@gmail.com

⁴ Centre for Computational and Systems Biology (COSBI), The Microsoft Research University of Trento, 38068 Rovereto, Italy; laura.caberlotto@evotec.com

⁵ Department of Biomedicine, Pharmazentrum, University of Basel, 4056 Basel, Switzerland; martin.gassmann@unibas.ch (M.G.); bernhard.bettler@unibas.ch (B.B.)

⁶ Department of Pharmacy and Biotechnology, Alma Mater Studiorum University of Bologna, 40126 Bologna, Italy; lucia.carboni4@unibo.it

* Correspondence: francesco.ferraguti@i-med.ac.at; Tel.: +43-512-900371204

† Current address: Aptuit, an Evotec Company, Via Fleming 4, 37135 Verona, Italy.

Abstract: The metabotropic glutamate receptor 1 (mGlu₁) plays a pivotal role in synaptic transmission and neuronal plasticity. Despite the fact that several interacting proteins involved in the mGlu₁ subcellular trafficking and intracellular transduction mechanisms have been identified, the protein network associated with this receptor in specific brain areas remains largely unknown. To identify novel mGlu₁-associated protein complexes in the mouse cerebellum, we used an unbiased tissue-specific proteomic approach, namely co-immunoprecipitation followed by liquid chromatography/tandem mass spectrometry analysis. Many well-known protein complexes as well as novel interactors were identified, including G-proteins, Homer, $\delta 2$ glutamate receptor, 14-3-3 proteins, and Na/K-ATPases. A novel putative interactor, KCTD12, was further investigated. Reverse co-immunoprecipitation with anti-KCTD12 antibodies revealed mGlu₁ in wild-type but not in KCTD12-knock-out homogenates. Freeze-fracture replica immunogold labeling co-localization experiments showed that KCTD12 and mGlu₁ are present in the same nanodomain in Purkinje cell spines, although at a distance that suggests that this interaction is mediated through interposed proteins. Consistently, mGlu₁ could not be co-immunoprecipitated with KCTD12 from a recombinant mammalian cell line co-expressing the two proteins. The possibility that this interaction was mediated via GABA_B receptors was excluded by showing that mGlu₁ and KCTD12 still co-immunoprecipitated from GABA_B receptor knock-out tissue. In conclusion, this study identifies tissue-specific mGlu₁-associated protein clusters including KCTD12 at Purkinje cell synapses.

Keywords: glutamate receptors; cerebellum; KCTD12; immunoprecipitation; proteomics



Citation: Mansouri, M.; Kremser, L.; Nguyen, T.-P.; Kasugai, Y.; Caberlotto, L.; Gassmann, M.; Sarg, B.; Lindner, H.; Bettler, B.; Carboni, L.; et al. Protein Networks Associated with Native Metabotropic Glutamate 1 Receptors (mGlu₁) in the Mouse Cerebellum. *Cells* **2023**, *12*, 1325. <https://doi.org/10.3390/cells12091325>

Academic Editor: Anna Pittaluga

Received: 17 March 2023

Revised: 28 April 2023

Accepted: 30 April 2023

Published: 5 May 2023



Copyright: © 2023 by the authors. Licensee MDPI, Basel, Switzerland. This article is an open access article distributed under the terms and conditions of the Creative Commons Attribution (CC BY) license (<https://creativecommons.org/licenses/by/4.0/>).

1. Introduction

Metabotropic glutamate receptors (mGlu_s) are members of class C G-protein coupled receptors (GPCRs) activated by glutamate, the major excitatory neurotransmitter in the central nervous system. These receptors are involved in many physiological functions including neuronal excitability, development, synaptic plasticity, and memory [1]. The eight members of this protein family are classified into three groups. Group I consists of mGlu₁ and mGlu₅, which share about 70% sequence homology and mainly couple to

Gαq. Group I mGluRs are selectively activated by (S)-3,5-dihydroxyphenylglycine and are mainly localized post-synaptically [2,3]. In the cerebellar cortex, mGlu₁ is highly expressed in Purkinje cells and a subset of interneurons, whereas mGlu₅ is expressed in Golgi and Lugaro cells and in deep cerebellar nuclei [4–7]. At glutamatergic synapses of Purkinje cells, mGlu₁ contributes to long-term depression (LTD), which is important for cerebellar learning mechanisms [8]. Gene-targeted deletion of mGlu₁ results in impaired LTD and severe ataxia [9,10]. This receptor also plays an important role in the elimination of multiple climbing fiber innervation to Purkinje cells during development [11,12]. These functions critically depend on the coupling of mGlu₁ to Gαq proteins [12,13]. In addition, mGlu₁ is involved in synaptic plasticity at GABAergic synapses such as rebound potentiation which is mediated by coupling of the receptors to Gαs [14]. A number of studies have shown that G-protein dependent as well as G-protein independent functional properties of mGlu₁ depend on their interaction with scaffolding and signaling proteins, including other GPCRs and ion-channels [15,16]. Alternative splicing at the mGlu₁ gene (*Grm1*) generates four variants, namely mGlu₁α, mGlu₁β, mGlu₁γ, and mGlu₁δ, which share a large part of the N-terminal sequence but differ primarily in their intracellular C-terminal domains [1]. The mGlu₁α isoform has the longest C-terminal domain and can physically interact with a variety of proteins through motifs that are not present in the shorter isoforms [17,18]. CFTR-associated ligand (aka Golgi-Associated PDZ And Coiled-Coil Motif-Containing Protein) [19], Homer proteins [20,21], Norbin (neurochondrin) [22,23], protein phosphatase 1C [24], Siah-1A [25], and Tamalin [26] are some of the signaling and scaffolding proteins that were reported to directly bind to mGlu₁α [15]. This isoform was also found to form functional complexes with the Gluδ2 receptor and the short Transient Receptor Potential Cation channel C3 (TRPC3) [27–31].

Most of our current knowledge about mGlu₁ interaction partners is obtained from affinity purifications or yeast two-hybrid screenings. In recent years, proteomic studies have emerged as a valuable tool for studying the co-assembly of proteins in native tissue. Proteomic approaches have the advantage of identifying stable and transient protein–protein interactions, defining native protein complexes, and finding novel interaction partners [32,33].

In the current study, we used a proteomic approach to identify protein complexes that are associated with mGlu₁α in the cerebellum. We immunoprecipitated mGlu₁α from mice cerebellar lysates and analyzed co-purified proteins by mass spectrometry. Using this approach, we identified multiple well-known as well as novel interactors and generated a mGlu₁ protein interaction network. We investigated a novel mGlu₁α interaction partner, namely the Potassium Channel Tetramerization Domain-containing protein 12 (KCTD12), a GABA_B receptor auxiliary subunit, using *in vivo* and *in vitro* methods. Our findings showed that mGlu₁ and KCTD12 co-exist in the same nanodomain in Purkinje cell spines, though their interaction does not depend on direct physical binding but most likely through interposed proteins.

2. Materials and Methods

2.1. Experimental Animals

For immunoprecipitations of mGlu₁α from the cerebellum, adult male and female C57BL/6N wild-type (WT) (n = 23), *Grm1*-knock-out (KO) (n = 7), BALB/c WT (n = 4), GABA_{B1} (n = 4), and GABA_{B2} (n = 4) KO mice were used. C57BL/6N WT (n = 3) and KCTD12-KO (n = 3) adult male and female mice were used to immunoprecipitate KCTD12 from the cerebellum.

The following mice were used: C57BL/6N (Charles River, Sulzfeld, Germany), *Grm1*-KO (gift from GlaxoSmithKline), GABA_{B1} KO [34], GABA_{B2} KO [35], Balb/c littermate, and KCTD12-KO mice [36]. Experimental procedures on animals were approved by the Austrian Animal Experimentation Ethics Board (GZ66.011/28-BrGT/2009) and by the Veterinary Office of Basel-Stadt and were in compliance with the European Convention for the Protection of Vertebrate Animals used for experimental and other scientific purposes, the

Animal Experiments Act 2012 (TVG 2012), and the EU Directive 2010/63/EU. The authors further attest that all efforts were made to minimize the number of animals used.

2.2. Antibodies and Vectors

Antibodies against mGlu₁α (Af811-1 and Af660-1) were purchased from Frontier Institute Co. Ltd. (Hokkaido, Japan) and KCTD12 antibodies were generated as previously reported [37].

The plasmid containing the open reading frame for the mouse mGlu₁α DNA and lentiviral particles packaged for mouse KCTD12 DNA was obtained from Genecopoeia (Rockville, MD, USA). The expression of KCTD12 was under the control of the cytomegalovirus (CMV) promoter and both the plasmid and lentiviral vectors contained the neomycin resistance gene. The plasmid containing the open reading frame for mouse GABA_{B2}-YFP DNA under the control of the CMV promoter was previously reported [38].

2.3. Immunoprecipitation of Proteins from Mouse Cerebellum (P2 Fraction)

To immunoprecipitate mGlu₁α and KCTD12 and mouse cerebella were dissected and pooled. Homogenization was performed in ice-cold 10 mM Tris-HCl, pH 7.4 buffer containing 320 mM sucrose, 1 mM phenylmethylsulphonyl fluoride, 1 mM NaF, 1 mM Na₃VO₄, and complete EDTA-free protease inhibitors (Roche, Vienna, Austria) using a motorized homogenizer (Sartorius, Göttingen, Germany) at a speed of 1400 rpm and 10 strokes. Lysates were centrifuged for 10 min at 1000× *g* and 4 °C to remove unbroken cells and tissue debris. This process was repeated 2 more times. Supernatants were collected and centrifuged for 40 min at 17,000× *g* at 4 °C. The pellet (P2 fraction) was resuspended in ice-cold 25 mM Tris-HCl, pH 7.4 buffer containing 1 mM NaF, 1 mM Na₃VO₄, and complete EDTA-free protease inhibitors. The protein concentration was determined by the Bradford protein assay using bovine serum albumin as the standard protein.

P2 samples were centrifuged for 30 min at 20,000× *g* and 4 °C. The pellet was suspended for 1 h in ice-cold 25 mM Tris-HCl, pH 7.4 buffer containing 0.5% sodium deoxycholate, 1% NP-40, 0.1% sodium dodecyl sulfate (SDS), 137 mM NaCl, 3 mM KCl, 1 mM phenylmethylsulfonyl fluoride, 1 mM NaF, 1 mM Na₃VO₄, and complete EDTA-free protease inhibitors. Detergent lysates were then centrifuged for 60 min at 20,000× *g* and 4 °C. The supernatant was aspirated carefully and incubated with primary antibodies (0.2 µg/100 µg proteins) for 2 h at 6 °C with constant rotation. Dynabeads Protein-A (Invitrogen, Waltham, MA, USA) were added at the ratio of 1 µL:20 µg of protein followed by incubation for 1 h at 6 °C. The immunoprecipitation eluates were obtained by heating the samples in 1× Laemmli buffer plus 20 mM dithiothreitol for 10 min at 70 °C and 5 min at 56 °C to prevent oligomerization.

2.4. Immunoblotting

Samples were loaded on NuPAGE Bis-Tris 4–12% precast gels and proteins were resolved at 80 V in MOPS SDS buffer. Proteins were transferred to a polyvinylidene difluoride membrane overnight at 150 mA, 6 °C. The membranes were stained with Ponceau-S for 10 min and incubated in 5% dry milk blocking solution for 1 h at room temperature. Membranes were then incubated in primary antibodies for 2–3 overnights and 6 °C (1:3000). Immunoreactive bands were detected by incubation in horseradish peroxidase-conjugated secondary antibodies (Invitrogen) followed by the ECL Prime reagent. Chemiluminescence was visualized with the Fusion SL-4 Vilber Lourmat imaging system (Peqlab, Erlangen, Germany).

2.5. Mass Spectrometry (LC–MS/MS) Analysis of Proteins

Eluates were lyophilized in a Christ RVC 2-18 concentrator and loaded on precast NuPAGE 4–12% Bis-Tris gels (Invitrogen). After 1.5 cm running in a MOPS SDS buffer, the gels were stained for 1 h in Coomassie R-250 at room temperature. Destaining was performed overnight in 40% methanol and 10% glacial acetic acid solution.

Protein bands were excised from gels and digested with trypsin obtained from porcine pancreas (Sigma-Aldrich, Vienna, Austria), as previously described [39]. Tryptic digests were analyzed using an UltiMate 3000 nano-HPLC system coupled to an LTQ Orbitrap XL mass spectrometer (Thermo Scientific, Bremen, Germany). The peptides were separated on a homemade fritless fused silica micro-capillary column (75 μm i.d. \times 280 μm o.d. \times 10 cm length) packed with 3 μm reversed phase C18 material (Reprosil). The solvent for HPLC was 0.1% formic acid (solvent A) and 0.1% formic acid in 85% acetonitrile (solvent B). The gradient profile was as follows: 0–2 min, 4% B; 2–55 min, 4–50% B; 55–60 min, 50–100% B; and 60–65 min, 100% B. The flow rate was 250 nL/min.

The LTQ Orbitrap XL mass spectrometer was operated in the data-dependent mode selecting the top 10 most abundant isotope patterns with a charge of 2+ or 3+ from the survey scan with an isolation window of 2 for the mass-to-charge ratio (m/z). Survey full scan MS spectra were acquired from 300 to 2000 m/z at a resolution of 60,000 with a maximum Injection Time (IT) of 20 ms and automatic gain control (AGC) target 1×10^6 . The selected isotope patterns were fragmented by collisional-induced dissociation (CID) with a normalized collision energy of 35 and a maximum injection time of 55 ms.

Data analysis was performed using Proteome Discoverer 1.3 (Thermo Scientific) with the search engine Sequest. The raw files were searched against the *Mus musculus* database (167,940 entries) extracted from the NCBI nr. The precursor and fragment mass tolerances were set to 10 ppm and 0.02 Da, respectively, and up to two missed cleavages were allowed. Carbamidomethylation of cysteine and oxidation of methionine were set as variable modifications. Peptide identifications were filtered at a 1% false discovery rate.

2.6. Generation of a Stable Cell Line Expressing KCTD12

HEK293 cells were seeded for 24 h and transduced with lentiviral particles containing KCTD12 DNA at a multiplicity of infection-10 and selected with G418 (600 $\mu\text{g}/\text{mL}$). After 48 h, the cells were trypsinized and transferred to a new dish. G418 was added to the medium for the next 3 passages until dead cells were sparse. From that stage onwards, cells were split regularly when almost 90% were confluent without adding G418 to the growth medium. Cells were maintained in an incubator at 37 $^{\circ}\text{C}$, 5% CO_2 , and 95% humidity. Confirmation of KCTD12 protein translation was obtained by Western blot and immunofluorescence.

2.7. Immunofluorescence

KCTD12-expressing cells were quickly washed with ice-cold PBS and fixed in ice-cold 4% paraformaldehyde for 45 min. Fixed cells were washed 3 times in tris-buffered saline followed by 1 h incubation in blocking solution at room temperature. Cells were incubated overnight with primary antibodies (rabbit anti-KCTD12 1:3000; guinea pig anti mGlu $_1\alpha$ 1:1000) at 6 $^{\circ}\text{C}$. Cells were washed three times with tris-buffered saline and incubated with secondary antibodies [Cy3 donkey-anti rabbit IgG 1:400 (Jackson ImmunoResearch, Ely, UK); Alexa 488-goat anti guinea pig IgG, 1:1000 (Invitrogen)] overnight at 6 $^{\circ}\text{C}$ in the dark. Cells were washed twice in tris-buffered saline, a coverslip was mounted using Vectashield, and analysis was performed using a Zeiss Axioimager M1 microscope equipped with a metal halide lamp.

2.8. Transient Transfection and Immunoprecipitation

Stable cell lines were transfected with plasmids containing the mGlu $_1\alpha$ DNA and the GABA $_B2$ -YFP DNA. DNA and lipofectamine (Invitrogen) were diluted in Optimem, mixed at a ratio of 1:3, and incubated for 20 min at room temperature. The mixtures were added to the growth medium and the cells were kept in an incubator for 72 h. The cells were washed with warm PBS and lysed in an ice-cold buffer used for immunoprecipitation. Lysates were centrifuged for 40 min at 17,000 $\times g$ and 4 $^{\circ}\text{C}$. The supernatant was aspirated carefully and KCTD12 was immunoprecipitated using a guinea pig polyclonal antibody raised against KCTD12 following the same protocol as described above.

2.9. Freeze-Fracture Replica Immunogold Labeling (FRIL)

FRIL was performed according to previously published procedures [40,41]. Two C57BL/6N WT and two KCTD12-KO mice were perfused transcardially for 10 min with a solution containing 1% paraformaldehyde and 15% of a saturated solution of picric acid in 0.1 M phosphate buffer at a rate of 5 mL/min. The brains were quickly extracted from the skull and the cerebellums were cut with a vibratome (Leica Microsystems VT1000S, Vienna, Austria) into 140 μ m thick coronal sections from where samples of the cerebellar cortex molecular layer (Crus 2 lobule) were dissected out under a stereomicroscope. The slices were cryoprotected in 30% glycerol in 0.1 M phosphate buffer and high-pressure frozen by means of an HPM 010 machine (Bal-Tec, Balzers, Liechtenstein). The frozen slices were then freeze-fractured at -115 °C and replicated with a first layer of carbon (5 nm), shadowed by platinum (2 nm), and followed by a second carbon layer (15 nm) in a freeze-etching BAF 060 device (Bal-Tec). After thawing, the tissue attached to replicas was digested with stirring at 80 °C overnight in SDS solubilization buffer for FRIL.

For immunogold labeling of replicas, blocking was performed first in a solution consisting of 5% bovine serum albumin and 0.1% Tween-20 in tris-buffered saline, pH 7.4 at room temperature. Replicas were then incubated in primary antibodies (guinea pig anti-KCTD12 1:90; rabbit anti mGlu₁ α 1:300) for 72 h at 6 °C. Following extensive washes and 1 h blocking, replicas were incubated with gold-conjugated secondary antibodies of 5 and 10 nm (British Biocell International, Cardiff, UK; BBI 1175; BBI 009076) for 48 h at 6 °C. Incubation of the primary and secondary antibodies was in a sequence with the antibodies for the detection of mGlu₁ α always incubated first. The specificity of the antibodies was tested on tissue obtained from KO mice as well as by omitting the primary antibody. Replicas were mounted on pioloform-coated mesh copper grids and examined with a Philips CM120 transmission electron microscope (Philips, Eindhoven, The Netherlands).

2.10. Network Construction

We constructed a Protein–Protein Interaction (PPI) network for immunoprecipitated proteins identified in all 6 replicate experiments. To obtain reliable protein interactions, we extracted only the validated interactions for mice. The mouse network was modelled using the 1-step neighbors of the putative interacting proteins with high confidence. We comprehensively merged the interactions from multiple interaction databases, including iRefIndex (<https://irefindex.vib.be>; accessed on 12 September 2022), Mentha (<https://mentha.uniroma2.it>; accessed on 12 September 2022), InnateDB-all (<https://www.innatedb.com>; accessed on 19 September 2022), EBI-GOA (<https://www.ebi.ac.uk/GOA/index>; accessed on 19 September 2022), MiNT (<https://mint.bio.uniroma2.it>; accessed on 12 September 2022), IMEX (<https://www.imexconsortium.org>; accessed on 19 September 2022), and IntAct (<https://www.ebi.ac.uk/intact/home>; accessed on 19 September 2022). Indeed, the seven interaction databases cover the mouse interactome. To ensure data quality, the constructed network consists only of non-redundant and validated protein interactions. To this aim, we extracted protein interactions from each database and then combined them into the final network after removing overlapping proteins. The network was visualized with the Cytoscape software 3.9.1 (<https://cytoscape.org> accessed on 19 September 2022).

2.11. Network Analysis

There is evidence that the functional importance of proteins might be inferred from their topological properties, specifically their key positions in the protein interaction network [42,43]. To gain information on the network and its participating proteins, two centrality indices were evaluated for each protein: the degree and betweenness. The degree centrality shows how many direct neighbors a node in the network connects to. A protein is considered as a hub in the network if its degree centrality is high. Betweenness shows the bridge role of a protein for other proteins in the network [44]. A protein presenting high betweenness centrality is an important connector in the network, playing a key mediator role. The degree centrality is measured by counting the neighborhood of a node in the

network, thus identifying network hubs. Betweenness is the centrality measure based on shortest-path calculations.

A given network $G(N,E)$ consists of a set of nodes (N) and a set of edges (E) between them. An edge e_{ij} connects node n_i with node n_j . In this paper, the extracted network is unweighted and undirected. In an undirected graph, e_{ij} and e_{ji} are considered identical. Therefore, the neighborhood \aleph_i for a node n_i is defined as its direct connected neighbors, as follows:

$$\aleph = \{n_j : e_{ij} \in E\} \quad (1)$$

The degree Di of a node is defined as the number of nodes $|\aleph_i|$ in its neighborhood \aleph_i .

The betweenness centrality is calculated based on the shortest paths. For each node n_k in the network, we counted the total number of shortest paths from node n_i to node n_j , called $p(v_i, v_j)$ as well as the number of those paths that pass through n_k , called $p(v_i, v_j, v_k)$. The betweenness $B(v_k)$ of a node v_k is defined as follows:

$$B(n_k) = \sum_{n_i \neq n_k \neq n_j} \frac{p(n_i, n_k, n_j)}{d(n_i, n_j)} \quad (2)$$

Pathway analysis and the identification of enriched GO terms were performed using DAVID and GOrilla based on the 10% highest scoring proteins in the network [45–47].

3. Results

3.1. Immunoprecipitation of mGlu1 α from Mouse Cerebellum

To identify protein complexes that can associate with mGlu1 α , we immunoprecipitated the receptor from mouse cerebellar extracts (Figure 1A). Pilot experiments were performed to determine the optimal conditions for immunoprecipitation. Two main conditions have been optimized: (1) solubilization and (2) the choice and concentration of antibody. Optimal detergent conditions were determined empirically by assessing the amount of native mGlu1 α extracted from cerebellar lysates by Western blot. Under our experimental conditions, a combination of 0.5% deoxycholate, 0.1% SDS, and 1% NP-40 was most effective in extracting mGlu1 α . Three different antibodies were tested for immunoprecipitation: a guinea pig polyclonal antibody raised against the amino acids 945–1127 (Af660-1) within the C-terminal region of mGlu1 α and two rabbit polyclonal antibodies raised against amino acid residues 945–1127 (Af811-1) or 1179–1199 (AB1551). Only the antibodies directed against the sequence 945–1127 were able to specifically immunoprecipitate mGlu1 and were used in subsequent experiments. A concentration of 0.2 μ g of antibody per 100 μ g of proteins resulted in the most efficient immunoprecipitation of the receptor. Three immunoprecipitation replicate experiments were then performed with antibody Af811-1 and three additional ones with antibody Af660-1. Immunoprecipitations from *Grm1*-KO cerebellar lysates were carried out as controls for both antibodies.

In the LC–MS/MS analysis, mGlu1 α was successfully identified in all six immunoprecipitation experiments from WT, but not from *Grm1*-KO animals. In all experiments, the highest SEQUEST score was indeed observed for mGlu1 α . The protein sequence coverage of the receptor was between 31.6 and 49.5% (Figure 1B,C; Table 1). The number of unique peptides specifically corresponding to mGlu1 α ranged from 7 to 11. Additional 19 to 28 peptides were in common between mGlu1 α and mGlu1 β (Table 1; Supplementary Table S1). mGlu1 β is a short alternatively spliced variant of the *Grm1* gene in which the last 318 amino acid residues of the mGlu1 α variant are replaced by 20 different residues [1]. Available evidence suggests that mGlu1 α and mGlu1 β variants heterodimerize both in vitro and in vivo [48–50] which affects receptor trafficking to the plasma membrane of Purkinje cell [46,47]. In line with these previous findings, we were able to identify specific mGlu1 β peptides in five out of six experiments, despite the fact that the specific portion of the mGlu1 β variant is quite short. Therefore, our results provide further support to the notion that mGlu1 α and mGlu1 β heterodimerize in Purkinje neurons.

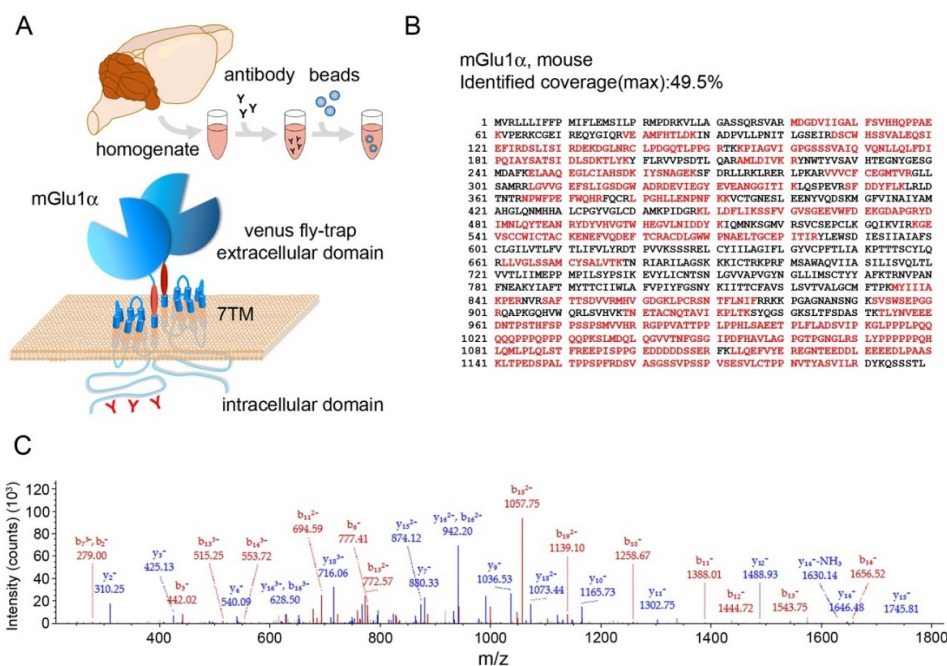


Figure 1. Multi-epitope affinity purification identifies native mGlu₁ in mouse cerebellar protein extracts. **(A)** Schematic of the immunoprecipitation procedure and of the mGlu₁α structure. **(B)** Primary mGlu₁α amino acid sequence. Red indicates the protein coverage of mGlu₁α identified by MS analysis. **(C)** MS/MS spectra of the mGlu₁ unique peptide YDYVHVGTWHEGVLNIDDYK. Monoisotopic m/z 808.38007 Da (−1.56 mmu/−1.93 ppm). MH⁺: 2423.12564 Da, RT: 32.51 min. Fragment match tolerance used for search: 0.8 Da. Fragments used for search: b; b-H₂O; b-NH₃; y; y-H₂O; and y-NH₃. Ion series: b (shown in red), y (shown in blue).

Table 1. Identification of mGlu₁α by LC-MS/MS in six immunoprecipitation experiments.

Coverage (%)	Unique Peptides ¹ (Number)	Peptides (Number)
35.11	11	33
31.61	7	29
43.20	10	34
49.54	11	39
46.79	11	37
31.61	8	27

¹ Peptides not shared with mGlu₁β.

3.2. mGlu1α Co-Immunoprecipitated Proteins

Proteomic analysis using the *Mus musculus* NCBIInr database with a 99% confidence threshold yielded hundreds of proteins from each experiment. Immunoglobulins, keratins, and proteins co-immunoprecipitated from lysates of *Grm1*-KO mice were considered as non-specific interacting proteins and, therefore, removed from the list of putative mGlu₁ interaction partners. We identified a total of 304 proteins in the data pooled from the six experiments (Supplementary Table S2).

Among the identified proteins, 25 proteins were consistently detected in all 6 replicate experiments (Table 2) and were, therefore, considered putative interacting proteins with a high confidence. Several of these proteins have been previously described as mGlu₁ interactor partners, such as Homer proteins, the G-protein α/o subunit, inositol 3-phosphate receptors, and Gluδ2, as well as protein kinase C and calcium/calmodulin-dependent protein kinase II (CaMKII) [1,20,51–53]. Other previously recognized mGlu₁ interactors were detected in this study, although they were not included in Table 2 because they were not identified in all six replicates. Among them, the G-protein α/q subunit, the predominant G-protein coupled to mGlu₁ [1], was positively detected in four experiments out of

six (Supplementary Table S3). Likewise, TRPC3 was also identified in four experiments (Supplementary Table S3) in agreement with previous reports establishing TRPC3 as a downstream effector of mGlu₁-dependent synaptic transmission in Purkinje cells [28]. Ca_v2.1 calcium channels were reported to interact with mGlu₁ in Purkinje neurons [54] and were among the co-immunoprecipitated proteins (Supplementary Table S2).

Table 2. mGlu₁ interacting proteins identified in all six immunoprecipitation experiments.

Protein ID	Protein Name	Gene ID	Unique Peptides (Number)	NCBI ID
P97772	metabotropic glutamate receptor 1	<i>Grm1</i>	48	NP_058672.1
P18872	guanine nucleotide-binding protein G(o) subunit α	<i>Gnao1</i>	11	NP_034438.1
P62874	guanine nucleotide-binding protein G(l)/G(s)/G(t) subunit β -1	<i>Gnb1</i>	6	NP_001153488.1
Q8BW86	ρ guanine nucleotide exchange factor 33	<i>Arhgef33</i>	14	NP_001138924.1
Q6PIC6	sodium/potassium-transporting ATPase subunit α -3	<i>Atp1a3</i>	26	NP_001361556.1
Q6PIE5	sodium/potassium-transporting ATPase subunit α -2	<i>Atp1a2</i>	14	NP_848492.1
P14094	sodium/potassium-transporting ATPase subunit β -1	<i>Atp1b1</i>	7	NP_033851.1
Q91V14	solute carrier family 12 member 5	<i>Slc12a5</i>	29	NP_001342409.1
P56564	excitatory amino acid transporter 1	<i>Slc1a3</i>	6	NP_683740.1
O35544	excitatory amino acid transporter 4	<i>Slc1a6</i>	7	NP_033226.1
Q61625	glutamate receptor ionotropic, δ -2	<i>Grid2</i>	20	NP_032193.1
Q99JP6	homer protein homolog 3	<i>Homer3</i>	14	NP_001139625.1
P16330	2',3'-cyclic-nucleotide 3'-phosphodiesterase	<i>Cnp</i>	10	NP_001139790.1
Q91VR2	ATP synthase subunit γ , mitochondrial	<i>Atp5c1</i>	6	NP_065640.2
Q8VEM8	phosphate carrier protein, mitochondrial	<i>Slc25a3</i>	5	NP_598429.1
P48962	ADP/ATP translocase 1	<i>Slc25a4</i>	3	NP_031476.3
P61982	14-3-3 protein γ	<i>Ywhag</i>	7	NP_061359.2
P68254	14-3-3 protein θ	<i>Ywhaq</i>	8	NP_035869.1
P11881	inositol 1,4,5-trisphosphate receptor type 1	<i>Itp1</i>	62	NP_034715.3
Q7TNC9	inositol polyphosphate-5-phosphatase A	<i>Inpp5a</i>	10	NP_898967.2
P63318	protein kinase C γ type	<i>Prkcg</i>	16	NP_035232.1
P28652	calcium/calmodulin-dependent protein kinase type II subunit β	<i>Camk2b</i>	4	NP_001167524.1
P35802	neuronal membrane glycoprotein M6-a	<i>Gpm6a</i>	2	NP_705809.1
P46097	synaptotagmin-2	<i>Syt2</i>	4	NP_001342655.1
Q6WVG3	BTB/POZ domain-containing protein KCTD12	<i>Kctd12</i>	9	NP_808383.3

We further detected mGlu₅, though only in one experiment, that was shown to form functional heterodimers with mGlu₁ [55,56] despite the fact that their colocalization is restricted to Golgi and Lugaro cells and deep nuclei in the adult rodent cerebellum [4–7]. GABA_B and GABA_A receptor subunits were also recovered (Supplementary Table S2), consistent with the identification of mGlu₁ also at GABAergic synapses [57,58].

Among the proteins identified with high confidence, we also detected novel putative interactors (Table 2). These included the ρ guanine nucleotide exchange factor 33 (RhoGEF33), excitatory amino acid transporters, 14-3-3 adapter proteins, Na⁺/K⁺ ATPase subunits, synaptotagmin-2 (Syt2), the K⁺/Cl⁻ cotransporter KCC2, and the KCTD12 protein. The KCTD family of proteins includes 21 members that share a common tetramerization T1 domain [59]. KCTD8, 12, 12b, and 16 form homo- and hetero-oligomers and directly bind to the GABA_{B2} receptor subunit via their T1 domains [38,60,61]. The expression of KCTD12 and 12b strongly desensitizes the GABA_B receptor response [62].

3.3. mGlu₁ Interactome

To gain further insight into the interactions between the identified and other neuronal proteins, we constructed a network based on validated interactions as available from the literature and collected in several databases (see Section 2.10). We constructed a network from the most reliably identified proteins (Table 2). The network had 643 nodes and 964 edges; the section centered on mGlu₁ is displayed in Figure 2. The highlighted proteins belong to the starting list of high-confidence interactors; they are endowed with high scores in the degree and/or betweenness centralities (Supplementary Table S4) to signify close interactions and important mediating roles. Out of the 304 proteins identified by LC-MS/MS analysis, in at least one of the experiments, 26.6% were present among the nodes of the network. Pathway and gene ontology (GO) enrichment analysis was carried

out on network proteins (Supplementary Tables S5 and S6). Pathway enrichment analysis, as expected, identified among the terms with highest score: glutamatergic synapse, protein–protein interaction at synapses and long term potentiation. Noteworthy, also circadian entrainment, the cGMP-PKG signaling pathway and neurexins and neuroligins showed high significance. GO term enrichment highlighted the known role of mGlu₁ in synaptic plasticity, glutamatergic signaling and locomotor behavior [63], but also regulation of Ca²⁺/Na⁺ antiporter activity and mitogen-activated protein kinases [64].

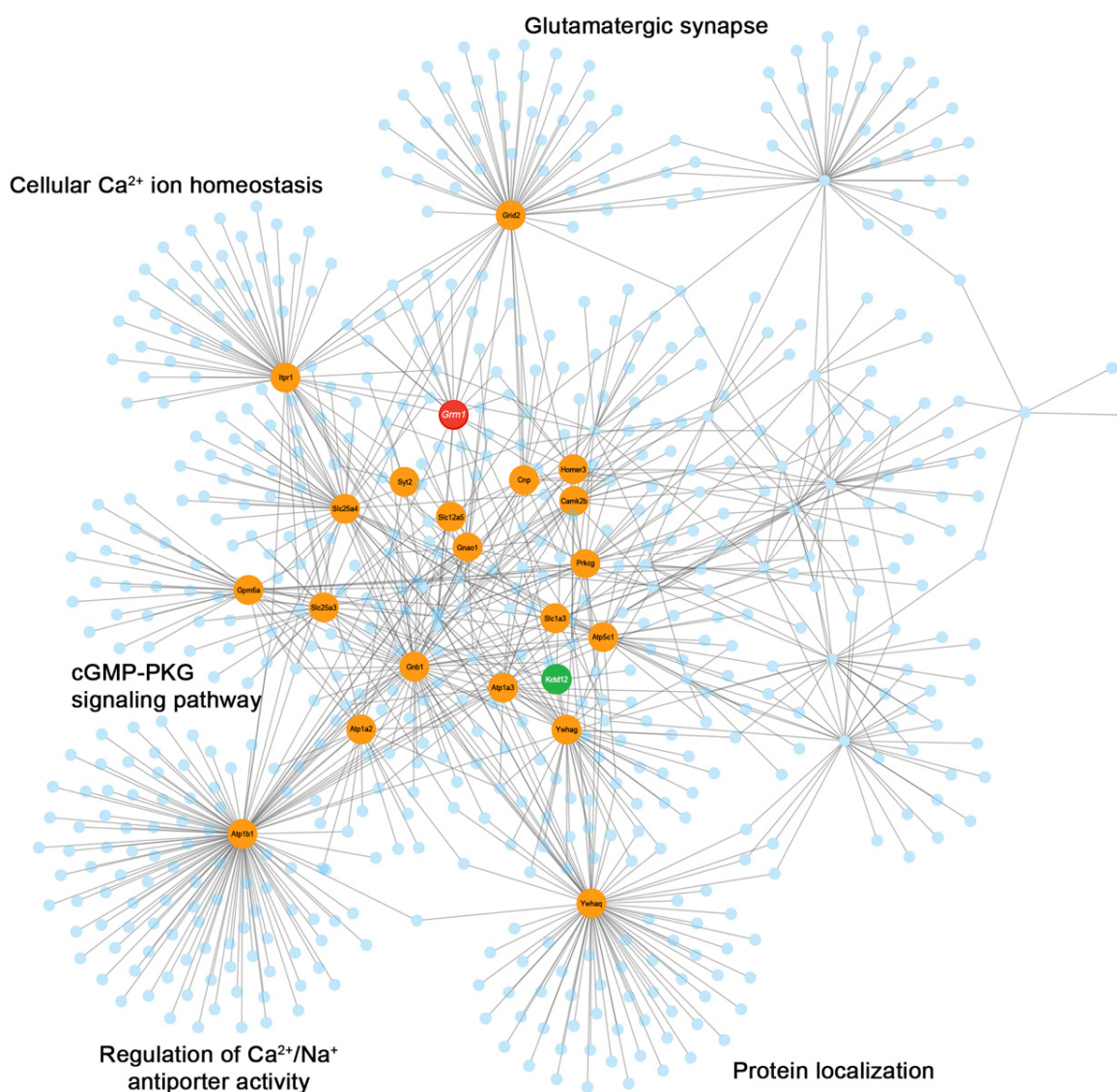


Figure 2. Protein network associated with mGlu₁ in mouse cerebellar synapses. The nodes represented by high-confidence mGlu₁ putative and established interactors are shown in orange, mGlu₁ is shown in red, and KCTD12 in green. A few GO-extracted functionalities are given at the side of protein communities having a high confidence mGlu₁ interactor as the starting protein.

3.4. Interaction between mGlu₁α and KCTD12 in the Cerebellum

We then focused on the putative interaction between mGlu₁α and KCTD12 because (1) KCTD12 directly interacts with the GABA_{B2} subunit of GABA_B receptors [38,62], which are also members of the class C GPCRs and share structural similarities with mGlu₁ [17]; (2) KCTD12 is highly expressed in the dendritic spines and shafts of Purkinje cells [37,62]; and (3) KCTD12 co-purifies G-protein βγ subunits even in the absence of GABA_{B2} [65]. Inter-

estingly, in our proteomic approach, G-protein $\beta\gamma$ subunits were also co-immunoprecipitated with mGlu $_1\alpha$.

At first, we performed co-immunoprecipitation experiments followed by Western blots using cerebellar lysates from WT, *Grm1*-KO, and KCTD12-KO mice. KCTD12 was consistently co-immunoprecipitated with mGlu $_1\alpha$ in WT but not *Grm1*-KO eluates (Figure 3). The co-assembly between the two proteins was further examined by reverse co-immunoprecipitation from cerebellar lysates of WT and KCTD12-KO mice. When KCTD12 was immunoprecipitated, bands corresponding to mGlu $_1\alpha$ (monomer around 145 kDa and dimer/multimer above 205 kDa) were also detected in WT but not KCTD12-KO eluates (Figure 3). However, the efficiency of mGlu $_1\alpha$ co-immunoprecipitation with KCTD12 appeared very low and might be due to the preferential and strong binding of KCTD12 to GABA $_B$ receptors. Taken together, these results support a direct or indirect interaction of mGlu $_1\alpha$ with KCTD12 in the cerebellum.

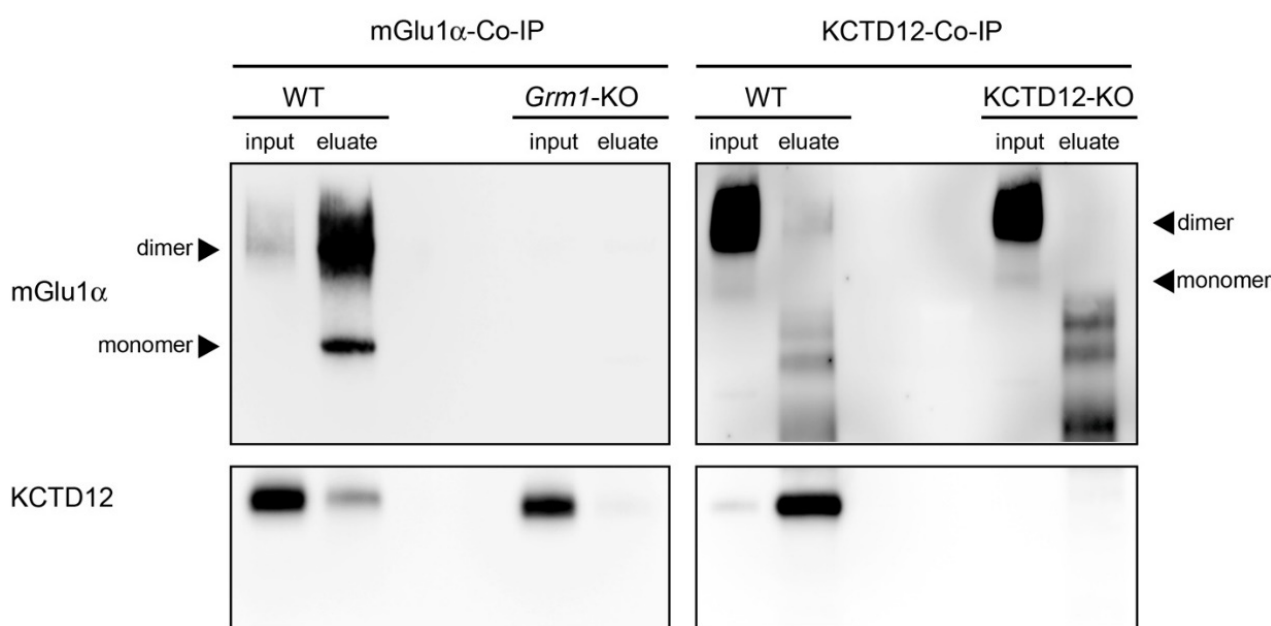


Figure 3. mGlu $_1\alpha$ and KCTD12 co-immunoprecipitants from the cerebellum. Left: mGlu $_1\alpha$ was immunoprecipitated from the cerebellum of WT and *Grm1*-KO mice using the anti-mGlu $_1\alpha$ antibody raised in guinea pigs and immunoblotted using anti-mGlu $_1\alpha$ (**top**) and anti-KCTD12 (**bottom**) antibodies raised in rabbit. Lanes: WT-input; WT-eluate; KO-input; KO-eluate. Right: KCTD12 was immunoprecipitated from the cerebellum of WT and KCTD12-KO mice using the anti-KCTD12 antibody raised in guinea pigs and immunoblotted using the anti-mGlu $_1\alpha$ raised (**top**) and anti KCTD12 (**bottom**) antibodies raised in rabbits. Lanes: WT-input; WT-eluate; KO-input; KO-eluate. Non-specific bands were detected between 90 and 70 kDa with the anti-mGlu $_1\alpha$ antibody in eluates of KCTD12-Co-IPs.

3.5. The Co-Existence of mGlu $_1\alpha$ and KCTD12 in the Same Microdomain of Cerebellar Purkinje Cell Dendritic Spines

Next, we studied the spatial relationship between mGlu $_1\alpha$ and KCTD12 in the mouse cerebellar cortex using the freeze-fracture replica immunogold labeling (FRIL) technique. Protoplasmic face immunogold labelling for both mGlu $_1\alpha$ and KCTD12 was observed at postsynaptic elements of Purkinje cells. At Purkinje cell spines, immunogold particles corresponding to KCTD12 were mainly found peri-synaptically (Figure 4A,B), similar to mGlu $_1\alpha$ [58,66]. At dendritic shafts, KCTD12 was also detected at extra-synaptic sites with or without mGlu $_1\alpha$ in close vicinity (Figure 4C). The nearest neighbor analysis confirmed that labeling for mGlu $_1\alpha$ and KCTD12 co-existed in a nano-domain in both dendritic spines and shafts of Purkinje cells (mean distance \pm s.e.m.: 26.70 \pm 2.0 nm for spines;

36.86 ± 3.44 nm for dendrites) (Figure 4D). The distance between gold particles detecting mGlu₁α was also analyzed (mean distance \pm s.e.m.: 19.73 ± 0.85 nm for spines; 22.90 ± 0.95 nm for dendrites), thus revealing that the distribution of their nearest neighbor distance was shorter when compared to gold particles detecting KCTD12 (two-sample Kolmogorov-Smirnov test, spines: $p = 0.0028$; dendrites: $p = 0.0001$) and that this is probably due to homodimerization (Figure 4D). The specificity of immunogold labeling was tested by labeling replicas obtained from mGlu₁-KO and KCTD12 KO cerebellum as well as omitting primary antibodies.

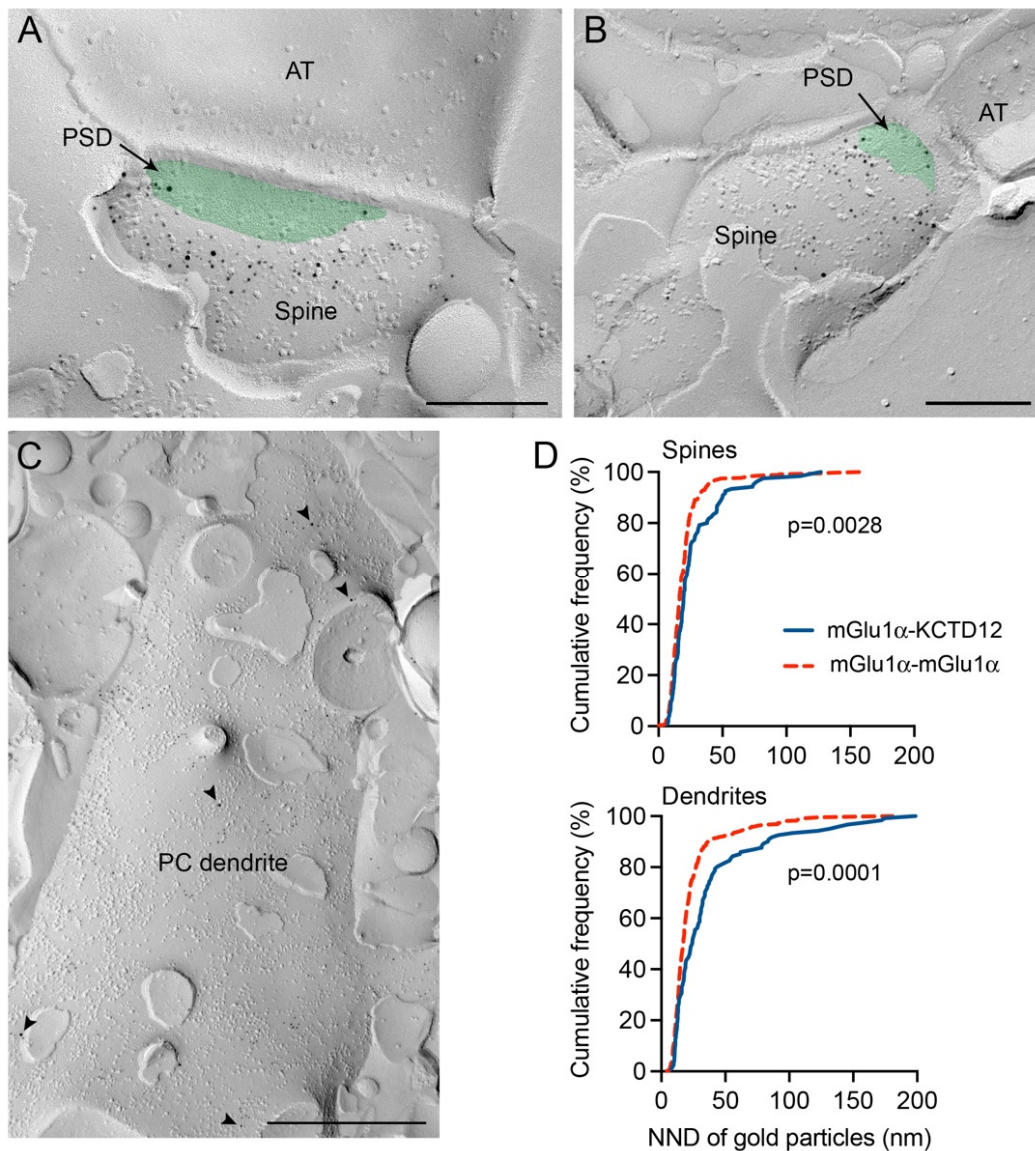


Figure 4. FRIL shows co-distribution of mGlu₁α and KCTD12 in the same nano-domain at dendritic spines and shafts of cerebellar Purkinje cells. (A,B) Electron micrographs showing co-localization of mGlu₁α (5 nm) and KCTD12 (10 nm) in spines. A pseudocolor (green) has been used to simplify the identification of the postsynaptic density (PSD). (C) A Purkinje cell dendrite shows KCTD12 labeling at extra-synaptic sites (arrowhead). (D) Cumulative distributions of the nearest neighbor distance (NND) of gold particles detecting mGlu₁α and KCTD12 in Purkinje cell spines and dendritic shafts. Abbreviations: AT, axon terminal; PC, Purkinje cell. Scale bars: (A,B) 200 nm and (C) 500 nm. Data were analyzed by means of the two-sample Kolmogorov-Smirnov Test. p values < 0.05 were considered significant.

3.6. *In Vitro* Analysis of the mGlu1 α –KCTD12 Interaction

To further examine the interaction between mGlu1 α and KCTD12, we adopted an *in vitro* approach. HEK293 cells stably over-expressing mouse KCTD12 were transiently transfected with a mouse mGlu1 α plasmid (Supplementary Figure S1). Since KCTD12 directly binds to the GABA_{B2} receptor subunit [62], cells were transfected with GABA_{B2} as a positive control. Mock-transfected cells were used as a negative control. KCTD12 was successfully immunoprecipitated from whole cell lysates of mock-transfected, mGlu1 α -transfected, and GABA_{B2}-transfected cells (Figure 5). However, there was no co-immunoprecipitation of mGlu1 α with KCTD12, whereas the GABA_{B2} receptor was detected in the co-immunoprecipitation (Figure 5). These findings suggest that the interaction between mGlu1 α and KCTD12 is not occurring via a direct binding but is mediated indirectly through additional proteins.

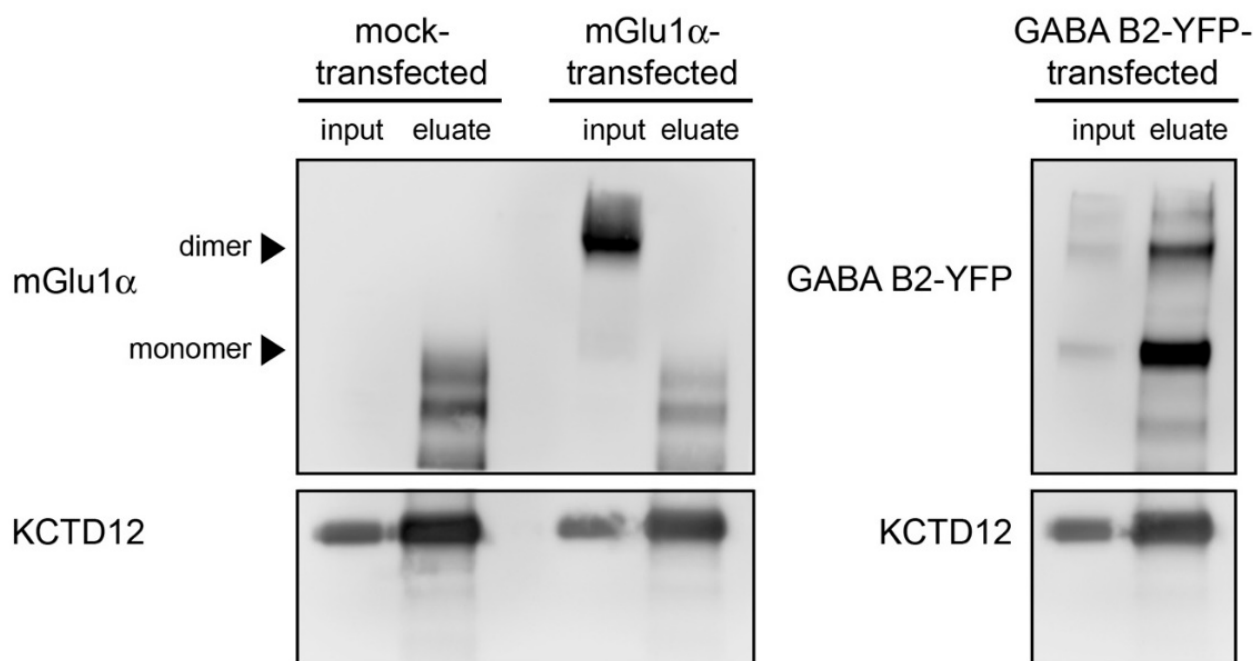


Figure 5. mGlu1 α and KCTD12 do not directly interact *in vitro*. KCTD12 was immunoprecipitated from KCTD12 cells that were not transfected, transfected with mGlu1 α , or transfected with GABA_{B2}-YFP plasmids. The anti-KCTD12 antibody raised in guinea pigs was used for immunoprecipitation and the anti-mGlu1 α (top left), anti-GABA_{B2} (top right), and anti-KCTD12 (bottom) antibodies raised in rabbit were used for immunoblots. Lanes are from whole cell lysates of mock-transfected-input; mock-transfected-eluate; mGlu1 α transfected-input; mGlu1 α transfected-eluate; GABA_{B2}-YFP transfected-input; and GABA_{B2}-YFP transfected-eluate. Non-specific bands were detected between 90 and 70 kDa with the anti-mGlu1 α antibody in eluates.

3.7. The mGlu1 α Receptor–KCTD12 Interaction Is Not Mediated by GABA_B Receptors

Since Purkinje cells abundantly express GABA_B receptors [67], we investigated whether the *in vivo* interaction between mGlu1 α and KCTD12 occurs through binding of KCTD12 to GABA_B receptors. We immunoprecipitated mGlu1 α from cerebellar lysates of WT, GABA_{B1}-KO, and GABA_{B2}-KO mice. If the interaction between mGlu1 α and KCTD12 were due to GABA_B receptors, then KCTD12 should not be detected in the immunoprecipitants of mGlu1 α from GABA_{B1}-KO and GABA_{B2}-KO lysates. However, a band corresponding to the molecular weight of KCTD12 was detected in mGlu1 α immunoprecipitants from both GABA_{B1}-KO and GABA_{B2}-KO lysates (Figure 6), suggesting that the interaction of mGlu1 α with KCTD12 is not mediated by GABA_B receptors.

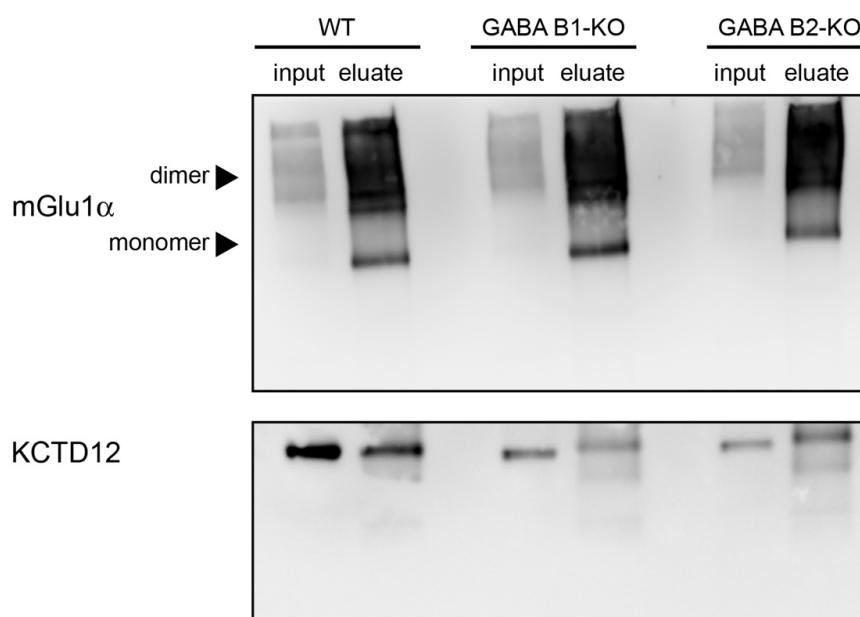


Figure 6. The interaction between the mGlu₁α and KCTD12 is not mediated by GABA_B receptors. mGlu₁α was immunoprecipitated from WT, GABA_{B1}-KO, and GABA_{B2}-KO cerebellar lysates. The anti-mGlu₁α antibody raised in guinea pigs was used for immunoprecipitation. The anti-mGlu₁α (**top**) and anti-KCTD12 (**bottom**) antibodies raised in rabbits were used for immunoblots. Lanes: WT-input; WT-eluate; GABA_{B1}-KO-input; GABA_{B1}-KO-eluate; GABA_{B2}-KO-input; GABA_{B2}-KO-eluate.

4. Discussion

In this study, we determined that the mGlu₁ interactome at mouse cerebellar synapses comprises 304 proteins forming a dense network involved in a number of neuronal functions including receptor trafficking, intracellular signaling, and synaptic plasticity. Using a highly conservative approach to select a small number of high confidence interacting partners, i.e., detected in all 6 experimental replicates, we could identify 25 proteins that interact directly or indirectly with mGlu₁, some of which were already known. Among the novel interactors, we focused on KCTD12 because of its direct binding to GABA_{B2} [62] which has strong structural similarities to mGlu₁ [17]. Taking a high-resolution imaging approach, we showed, by means of immuno-electron microscopy, that KCTD12 and mGlu₁α were present in the same nanodomain in Purkinje cell spines. However, using a recombinant mammalian cell line co-expressing both proteins, we were unable to co-immunoprecipitate mGlu₁α with KCTD12. We excluded the possibility that the GABA_B receptor mediates the interaction between KCTD12 and mGlu₁α. Taken together, our findings suggest that KCTD12 interacts with mGlu₁α indirectly, possibly via G-protein subunits [65] or other proteins that interact with mGlu₁α.

We adopted a proteomic approach based on co-immunoprecipitation and LC-MS/MS. The isolation of protein complexes from brain tissues using immunoprecipitation coupled to MS provides a significant advantage over other methods to detect protein–protein interactions as it allows for the analysis of complexes within native physiological cellular domains. However, proteomic results can be confounded by false positive interactions due to antibody cross-reactivity. To overcome this problem, we have used tissue obtained from *Grm1*-KO mice as control samples. This strategy helped us to ensure the selection of truly interacting proteins expressed in the mouse cerebellum.

Using only interacting partners with high confidence, we built a protein interaction network that had over 600 nodes. However, we are aware that many bona fide interacting proteins might have been excluded from such a conservative approach. Our findings show that approximately one-fourth of the proteins identified by our proteomic approach overlapped with the network proteins, on one hand supporting the validity of the network

for cerebellar synapses also. On the other hand, our data indicate a molecular complexity of the cerebellar mGlu₁ interactome greater than the models generated based on the currently available databases and the extant literature. Future studies can avail the additional identified proteins to expand our knowledge on the mGlu₁ interactome both in terms of its fundamental as well as synapse-specific molecular components.

Our proteomic approach identified several proteins already described as mGlu₁ interactor partners, such as Homer proteins that directly interact with the C-terminal domain of group I mGlu_s [20,68]. Likewise, a number of effectors involved in the classical signaling pathway of group I mGlu_s, namely the hydrolysis of phosphoinositides and release of Ca²⁺ from intracellular stores, were detected by our LC-MS/MS analysis of co-immunoprecipitated proteins. These effectors included the inositol 3-phosphate receptor type 1, phospholipase Cβ4, calmodulin, protein kinase Cγ, and TRPC3 besides the G-protein αq and αi subunits. Amid the mGlu₁ high confidence interacting proteins, we also detected subunits of CaMKII, a highly abundant serine/threonine kinase in the post-synaptic density of Purkinje cells. This finding is consistent with studies showing the presence of multiple CaMKII consensus motifs in the mGlu₁ C-terminal domain [69–71] and their phosphorylation by CaMKII through a direct interaction [70]. As for the interactors, we identified members of the 14-3-3 protein family, small-size proteins (27–32 kDa) highly enriched in the brain and involved in multiple cellular signaling events by functioning as adaptors and scaffolds. The 14-3-3 proteins have been reported as important modulators of glutamatergic synapses, potentially integrating multiple signaling pathways [72]. They interact with several G-protein coupled receptors, including GABA_B and α2-adrenergic receptors [73] but interactions with mGlu₁ have never been reported thus far. Nevertheless, a 14-3-3 isoform was shown to mediate the group I mGlu-agonist-induced down-regulation of KCNK3 potassium channel activity through protein kinase C [74], thus supporting the hypothesis of a role in mGlu₁ signaling. Although with low efficiency (in only one experiment, but the one yielding the highest number of interactors), we detected mGlu₅ among the interaction partners of mGlu₁. In the adult rodent cerebellum, only Golgi and Lugaro cells and neurons in the deep nuclei were shown to co-express mGlu₁ and mGlu₅ [4–7]. Group I mGlu_s are known to form heterodimers in recombinant systems and cultured neurons [55,56] and to co-purify from brain membranes [55,75]. While the existence of functional mGlu₁/mGlu₅ heterodimers in native tissue remains to be unambiguously demonstrated, our findings provide further support to this notion. The low efficiency may be compatible with the restricted co-expression of these two receptors in just a few cerebellar cell types.

In our experiments, we consistently detected a high number of unique peptides for the neuron-specific α3 catalytic subunit as well as other subunits of the Na⁺/K⁺-ATPase, which contributes to maintaining the polarity of mammalian cells by actively exporting Na⁺ and importing K⁺ [76]. Despite the fact that the Na⁺/K⁺-ATPase was previously shown to interact with glutamate transporters and ionotropic receptors [76], possible non-specific co-immunoprecipitation cannot be ruled out because of its very high expression on the neuronal plasma membranes. Among the newly discovered interactors, RhoGEF33, which belongs to a membrane-bound protein family of upstream regulators of Rho GTPases, is involved in different cellular processes including GPCR downstream signaling. The role of RhoGEF33 in relation to mGlu₁ may depend on its Rho GTPase function [77] involved in the regulation of synaptic structure and efficacy [78].

Among the novel putative interactors identified in our study, we focused on KCTD12 because of its direct binding to the GABA_{B2} receptor subunit [62] which has structural similarities to mGlu_s [17]. We reasoned that KCTD12 could similarly interact with mGlu₁ and regulate its signaling. Indeed, we were able to co-immunoprecipitate KCTD12 using antibodies against mGlu₁α. Reverse co-immunoprecipitation experiments similarly allowed the detection of mGlu₁α, although with lower efficiency. In addition, we showed that mGlu₁α and KCTD12 colocalize in the same nanodomain in Purkinje cell spines, strengthening the idea of a functional interaction in neurons *in vivo*. However, our nearest

neighbor analysis suggested that the distance between KCTD12 and mGlu₁α was incompatible with a direct physical interaction. Consistent with this hypothesis, we were unable to co-immunoprecipitate mGlu₁α with KCTD12 from HEK293 cell extracts expressing these two proteins. Previous studies reported a functional interaction between mGlu₁α and GABA_B receptors at Purkinje cell synapses [79,80] and showed that the activation of GABA_B receptors facilitates the mGlu₁-mediated LTD induction [51,80,81]. Furthermore, the two receptors were shown to co-immunoprecipitate from cerebellar extracts [51,79]. However, their interaction was shown to be indirect and mediated via Gβγ subunits released upon GABA_B receptor activation [82]. In line with these findings, we observed that KCTD12 was co-immunoprecipitated with the mGlu₁α even in the absence of the GABA_{B1} and GABA_{B2} receptor subunits, suggesting that the interaction between KCTD12 and mGlu₁α is independent of GABA_B receptors. A likely candidate to mediate the interaction between mGlu₁α and KCTD12 is the Gβ subunit of the G protein. KCTD12 also binds to Gβ [38] independently of GABA_B receptors [65]. It is, therefore, conceivable that mGlu₁ binds G proteins bound to KCTD12. This would also explain the weak co-immunoprecipitation of mGlu₁ with anti-KCTD12 antibodies. Future studies should explore whether Gβ subunits do indeed mediate this interaction.

Irrespective of the interaction mechanism between mGlu₁α and KCTD12, a still open question is the potential functional role of this interaction. KCTD12 mediates fast GABA_B receptor desensitization through its binding to the activated Gβγ subunits [65], thereby uncoupling them from the inwardly rectifying K⁺ (GIRK or Kir3) and voltage-gated Ca²⁺ channels (VGCCs) modulated by GABA_B receptor activation [62]. It can be surmised that KCTD12 similarly modulates mGlu₁ complex postsynaptic responses. In Purkinje cells, both VGCCs, namely Ca_v2.1 and Ca_v3.1 [54,83], and potassium channels [84,85] were shown to functionally interact with mGlu₁. KCTD12 may thus regulate mGlu₁α-mediated responses through these channels. In this respect, it is interesting to note that the related KCTD8 and KCTD12b proteins were shown to directly bind to and co-localize with Cav2.3 channels at the presynaptic zone in projections from the medial habenula where they modulate neurotransmitter release [86]. Future studies will be necessary to clarify the functional significance of the mGlu₁α–KCTD12 interaction.

5. Conclusions

The mGlu₁ interactome presented here serves as a molecular framework for further exploring the signaling, trafficking, and involvement in the cerebellar function of this receptor. Some of the proteins identified by our proteomic approach are novel putative interactors whereas others were already known to interact directly or indirectly with mGlu₁. Among the novel interactors, we focused on KCTD12 and showed that it coexists with mGlu₁α in the same nanodomain in Purkinje cell spines. However, biochemical analyses suggested an indirect interaction via additional proteins that warrants follow-up functional investigations.

Supplementary Materials: The following supporting information can be downloaded at: <https://www.mdpi.com/article/10.3390/cells12091325/s1>, Figure S1: Overexpression of mouse KCTD12 and mGlu₁α in HEK293 cells; Table S1: mGlu₁ peptides identified by LC–MS/MS in six immunoprecipitation experiments; Table S2: complete list of proteins identified in immunoprecipitation experiments; Table S3: list of proteins identified in 4 out of 6 immunoprecipitation replicate experiments; Table S4: list of nodes in the constructed network; Table S5: Pathway enrichment analysis of network proteins; Table S6: GO enrichment.

Author Contributions: Conceptualization, B.B., F.F. and M.M.; methodology, L.C. (Laura Caberlotto), L.K., M.G., M.M., T.-P.N. and Y.K.; validation, L.C. (Lucia Carboni), L.K., M.G. and M.M.; formal analysis, B.S., L.C. (Laura Caberlotto), L.K., M.M., T.-P.N. and Y.K.; investigation, L.K., M.G., M.M. and Y.K.; resources, B.B. and F.F.; data curation, L.C. (Lucia Carboni) and F.F.; writing F.F., L.C. (Lucia Carboni) and M.M.; supervision, B.B., F.F. and H.L.; project administration, F.F.; funding acquisition, F.F. and B.B. All authors have read and agreed to the published version of the manuscript.

Funding: This research was funded by the Austrian Science Fund grant no. W012060-10 and I2220 to F.F. and by the Swiss National Science Foundation Grant No. 31003A-152970 to B.B.

Institutional Review Board Statement: Experimental procedures on animals were approved by the Austrian Animal Experimentation Ethics Board (GZ66.011/83-BrGT/2005 and GZ66.011/28-BrGT/2009) and the National Institute for Physiological Science's Animal Care and Use Committee and were in accordance with directives of the French Ministry of Agriculture, in compliance with both the European Convention for the Protection of Vertebrate Animals used for Experimental and Other Scientific Purposes (ETS no. 123) and the European Communities Council Directive of 24 November 1986 (86/609/EEC).

Informed Consent Statement: Not applicable.

Data Availability Statement: Proteomic data are available via ProteomeXchange with the identifier PXD040886.

Acknowledgments: The authors acknowledge the excellent technical support of Sabine Schönherr and that of the Protein Core Facility of the Medical University of Innsbruck.

Conflicts of Interest: The authors declare no conflict of interest.

References

1. Ferraguti, F.; Crepaldi, L.; Nicoletti, F. Metabotropic glutamate 1 receptor: Current concepts and perspectives. *Pharmacol. Rev.* **2008**, *60*, 536–581. [[CrossRef](#)] [[PubMed](#)]
2. Niswender, C.M.; Conn, P.J. Metabotropic glutamate receptors: Physiology, pharmacology, and disease. *Annu. Rev. Pharmacol. Toxicol.* **2010**, *50*, 295–322. [[CrossRef](#)] [[PubMed](#)]
3. Ferraguti, F.; Shigemoto, R. Metabotropic glutamate receptors. *Cell Tissue Res.* **2006**, *326*, 483–504. [[CrossRef](#)] [[PubMed](#)]
4. Martin, L.J.; Blackstone, C.D.; Haganir, R.L.; Price, D.L. Cellular localization of a metabotropic glutamate receptor in rat brain. *Neuron* **1992**, *9*, 259–270. [[CrossRef](#)] [[PubMed](#)]
5. Shigemoto, R.; Nakanishi, S.; Mizuno, N. Distribution of the mRNA for a metabotropic glutamate receptor (mGluR1) in the central nervous system: An in situ hybridization study in adult and developing rat. *J. Comp. Neurol.* **1992**, *322*, 121–135. [[CrossRef](#)]
6. Shigemoto, R.; Mizuno, N. Chapter III Metabotropic glutamate receptors—immunocytochemical and in situ hybridization analyses. In *Handbook of Chemical Neuroanatomy*; Elsevier: Amsterdam, The Netherlands, 2000; pp. 63–98. [[CrossRef](#)]
7. Négyessy, L.; Vidnyánszky, Z.; Kuhn, R.; Knöpfel, T.; Görcs, T.J.; Hámori, J. Light and electron microscopic demonstration of mGluR5 metabotropic glutamate receptor immunoreactive neuronal elements in the rat cerebellar cortex. *J. Comp. Neurol.* **1997**, *385*, 641–650. [[CrossRef](#)]
8. Ito, M. Cerebellar circuitry as a neuronal machine. *Prog. Neurobiol.* **2006**, *78*, 272–303. [[CrossRef](#)]
9. Aiba, A.; Chen, C.; Herrup, K.; Rosenmund, C.; Stevens, C.F.; Tonegawa, S. Reduced hippocampal long-term potentiation and context-specific deficit in associative learning in mGluR1 mutant mice. *Cell* **1994**, *79*, 365–375. [[CrossRef](#)]
10. Conquet, F.; Bashir, Z.I.; Davies, C.H.; Daniel, H.; Ferraguti, F.; Bordi, F.; Franz-Bacon, K.; Reggiani, A.; Matarese, V.; Condé, F. Motor deficit and impairment of synaptic plasticity in mice lacking mGluR1. *Nature* **1994**, *372*, 237–243. [[CrossRef](#)]
11. Kano, M.; Hashimoto, K.; Kurihara, H.; Watanabe, M.; Inoue, Y.; Aiba, A.; Tonegawa, S. Persistent multiple climbing fiber innervation of cerebellar Purkinje cells in mice lacking mGluR1. *Neuron* **1997**, *18*, 71–79. [[CrossRef](#)]
12. Kano, M.; Hashimoto, K.; Tabata, T. Type-1 metabotropic glutamate receptor in cerebellar Purkinje cells: A key molecule responsible for long-term depression, endocannabinoid signalling and synapse elimination. *Philos. Trans. R. Soc. Lond. B. Biol. Sci.* **2008**, *363*, 2173–2186. [[CrossRef](#)]
13. Ichise, T.; Kano, M.; Hashimoto, K.; Yanagihara, D.; Nakao, K.; Shigemoto, R.; Katsuki, M.; Aiba, A. mGluR1 in cerebellar Purkinje cells essential for long-term depression, synapse elimination, and motor coordination. *Science* **2000**, *288*, 1832–1835. [[CrossRef](#)]
14. Sugiyama, Y.; Kawaguchi, S.; Hirano, T. mGluR1-mediated facilitation of long-term potentiation at inhibitory synapses on a cerebellar Purkinje neuron. *Eur. J. Neurosci.* **2008**, *27*, 884–896. [[CrossRef](#)]
15. Enz, R. Metabotropic glutamate receptors and interacting proteins: Evolving drug targets. *Curr. Drug Targets* **2012**, *13*, 145–156. [[CrossRef](#)]
16. Kalinowska, M.; Francesconi, A. Group I Metabotropic Glutamate Receptor Interacting Proteins: Fine-Tuning Receptor Functions in Health and Disease. *Curr. Neuropharmacol.* **2016**, *14*, 494–503. [[CrossRef](#)]
17. Pin, J.-P.; Bettler, B. Organization and functions of mGlu and GABA_B receptor complexes. *Nature* **2016**, *540*, 60–68. [[CrossRef](#)]
18. Suh, Y.H.; Chang, K.; Roche, K.W. Metabotropic glutamate receptor trafficking. *Mol. Cell. Neurosci.* **2018**, *91*, 10–24. [[CrossRef](#)]
19. Zhang, J.; Cheng, S.; Xiong, Y.; Ma, Y.; Luo, D.; Jeromin, A.; Zhang, H.; He, J. A novel association of mGluR1a with the PDZ scaffold protein CAL modulates receptor activity. *FEBS Lett.* **2008**, *582*, 4117–4124. [[CrossRef](#)]
20. Tu, J.C.; Xiao, B.; Yuan, J.P.; Lanahan, A.A.; Loeffert, K.; Li, M.; Linden, D.J.; Worley, P.F. Homer binds a novel proline-rich motif and links group 1 metabotropic glutamate receptors with IP3 receptors. *Neuron* **1998**, *21*, 717–726. [[CrossRef](#)]

21. Xiao, B.; Tu, J.C.; Worley, P.F. Homer: A link between neural activity and glutamate receptor function. *Curr. Opin. Neurobiol.* **2000**, *10*, 370–374. [[CrossRef](#)]
22. Wang, H.; Westin, L.; Nong, Y.; Birnbaum, S.; Bendor, J.; Brismar, H.; Nestler, E.; Aperia, A.; Flajolet, M.; Greengard, P. Norbin is an endogenous regulator of metabotropic glutamate receptor 5 signaling. *Science* **2009**, *326*, 1554–1557. [[CrossRef](#)] [[PubMed](#)]
23. Ojha, P.; Pal, S.; Bhattacharyya, S. Regulation of Metabotropic Glutamate Receptor Internalization and Synaptic AMPA Receptor Endocytosis by the Postsynaptic Protein Norbin. *J. Neurosci.* **2022**, *42*, 731–748. [[CrossRef](#)] [[PubMed](#)]
24. Croci, C.; Sticht, H.; Brandstätter, J.H.; Enz, R. Group I metabotropic glutamate receptors bind to protein phosphatase 1C. Mapping and modeling of interacting sequences. *J. Biol. Chem.* **2003**, *278*, 50682–50690. [[CrossRef](#)] [[PubMed](#)]
25. Moriyoshi, K.; Iijima, K.; Fujii, H.; Ito, H.; Cho, Y.; Nakanishi, S. Seven in absentia homolog 1A mediates ubiquitination and degradation of group 1 metabotropic glutamate receptors. *Proc. Natl. Acad. Sci. USA* **2004**, *101*, 8614–8619. [[CrossRef](#)]
26. Pandey, S.; Ramsakha, N.; Sharma, R.; Gulia, R.; Ojha, P.; Lu, W.; Bhattacharyya, S. The post-synaptic scaffolding protein tamalin regulates ligand-mediated trafficking of metabotropic glutamate receptors. *J. Biol. Chem.* **2020**, *295*, 8575–8588. [[CrossRef](#)]
27. Uemura, T.; Mori, H.; Mishina, M. Direct interaction of GluRδ2 with Shank scaffold proteins in cerebellar Purkinje cells. *Mol. Cell. Neurosci.* **2004**, *26*, 330–341. [[CrossRef](#)]
28. Hartmann, J.; Dragicevic, E.; Adelsberger, H.; Henning, H.A.; Sumser, M.; Abramowitz, J.; Blum, R.; Dietrich, A.; Freichel, M.; Flockerzi, V.; et al. TRPC3 channels are required for synaptic transmission and motor coordination. *Neuron* **2008**, *59*, 392–398. [[CrossRef](#)]
29. Hartmann, J.; Henning, H.A.; Konnerth, A. mGluR1/TRPC3-mediated Synaptic Transmission and Calcium Signaling in Mammalian Central Neurons. *Cold Spring Harb. Perspect. Biol.* **2011**, *3*, a006726. [[CrossRef](#)]
30. Bockaert, J.; Perroy, J.; Bécamel, C.; Marin, P.; Fagni, L. GPCR interacting proteins (GIPs) in the nervous system: Roles in physiology and pathologies. *Annu. Rev. Pharmacol. Toxicol.* **2010**, *50*, 89–109. [[CrossRef](#)]
31. Kato, A.S.; Knierman, M.D.; Siuda, E.R.; Isaac, J.T.R.; Nisenbaum, E.S.; Brecht, D.S. Glutamate Receptor 2 Associates with Metabotropic Glutamate Receptor 1 (mGluR1), Protein Kinase C, and Canonical Transient Receptor Potential 3 and Regulates mGluR1-Mediated Synaptic Transmission in Cerebellar Purkinje Neurons. *J. Neurosci.* **2012**, *32*, 15296–15308. [[CrossRef](#)]
32. Fingleton, E.; Li, Y.; Roche, K.W. Advances in Proteomics Allow Insights Into Neuronal Proteomes. *Front. Mol. Neurosci.* **2021**, *14*, 647451. [[CrossRef](#)]
33. Van Gelder, C.A.G.H.; Altelaar, M. Neuroproteomics of the synapse: Subcellular quantification of protein networks and signaling dynamics. *Mol. Cell. Proteomics* **2021**, *20*, 100087. [[CrossRef](#)]
34. Schuler, V.; Lüscher, C.; Blanchet, C.; Klix, N.; Sansig, G.; Klebs, K.; Schmutz, M.; Heid, J.; Gentry, C.; Urban, L.; et al. Epilepsy, hyperalgesia, impaired memory, and loss of pre- and postsynaptic GABA_B responses in mice lacking GABA_{B(1)}. *Neuron* **2001**, *31*, 47–58. [[CrossRef](#)]
35. Gassmann, M.; Shaban, H.; Vigot, R.; Sansig, G.; Haller, C.; Barbieri, S.; Humeau, Y.; Schuler, V.; Müller, M.; Kinzel, B.; et al. Redistribution of GABA_{B(1)} protein and atypical GABA_B responses in GABA_{B(2)}-deficient mice. *J. Neurosci.* **2004**, *24*, 6086–6097. [[CrossRef](#)]
36. Cathomas, F.; Stegen, M.; Sigrist, H.; Schmid, L.; Seifritz, E.; Gassmann, M.; Bettler, B.; Pryce, C.R. Altered emotionality and neuronal excitability in mice lacking KCTD12, an auxiliary subunit of GABA_B receptors associated with mood disorders. *Transl. Psychiatry* **2015**, *5*, e510. [[CrossRef](#)]
37. Metz, M.; Gassmann, M.; Fakler, B.; Schaeren-Wiemers, N.; Bettler, B. Distribution of the auxiliary GABA_B receptor subunits KCTD8, 12, 12b, and 16 in the mouse brain. *J. Comp. Neurol.* **2011**, *519*, 1435–1454. [[CrossRef](#)]
38. Fritzius, T.; Turecek, R.; Seddik, R.; Kobayashi, H.; Tiao, J.; Rem, P.D.; Metz, M.; Kralikova, M.; Bouvier, M.; Gassmann, M.; et al. KCTD hetero-oligomers confer unique kinetic properties on hippocampal GABA_B receptor-induced K⁺ currents. *J. Neurosci.* **2017**, *37*, 1162–1175. [[CrossRef](#)]
39. Faserl, K.; Chetwynd, A.J.; Lynch, I.; Thorn, J.A.; Lindner, H.H. Corona Isolation Method Matters: Capillary Electrophoresis Mass Spectrometry Based Comparison of Protein Corona Compositions Following On-Particle versus In-Solution or In-Gel Digestion. *Nanomaterials* **2019**, *9*, 898. [[CrossRef](#)]
40. Kasugai, Y.; Vogel, E.; Hörtnagl, H.; Schönherr, S.; Paradiso, E.; Hauschild, M.; Göbel, G.; Milenkovic, I.; Peterschmitt, Y.; Tasan, R.; et al. Structural and Functional Remodeling of Amygdala GABAergic Synapses in Associative Fear Learning. *Neuron* **2019**, *104*, 781–794.e4. [[CrossRef](#)]
41. Schönherr, S.; Seewald, A.; Kasugai, Y.; Bosch, D.; Ehrlich, I.; Ferraguti, F. Combined Optogenetic and Freeze-fracture Replica Immunolabeling to Examine Input-specific Arrangement of Glutamate Receptors in the Mouse Amygdala. *J. Vis. Exp.* **2016**. [[CrossRef](#)]
42. Zotenko, E.; Mestre, J.; O’Leary, D.P.; Przytycka, T.M. Why do hubs in the yeast protein interaction network tend to be essential: Reexamining the connection between the network topology and essentiality. *PLoS Comput. Biol.* **2008**, *4*, e1000140. [[CrossRef](#)]
43. Zhang, S.; Jin, G.; Zhang, X.-S.; Chen, L. Discovering functions and revealing mechanisms at molecular level from biological networks. *Proteomics* **2007**, *7*, 2856–2869. [[CrossRef](#)] [[PubMed](#)]
44. Joy, M.P.; Brock, A.; Ingber, D.E.; Huang, S. High-betweenness proteins in the yeast protein interaction network. *J. Biomed. Biotechnol.* **2005**, *2005*, 96–103. [[CrossRef](#)] [[PubMed](#)]

45. Sherman, B.T.; Hao, M.; Qiu, J.; Jiao, X.; Baseler, M.W.; Lane, H.C.; Imamichi, T.; Chang, W. DAVID: A web server for functional enrichment analysis and functional annotation of gene lists (2021 update). *Nucleic Acids Res.* **2022**, *50*, W216–W221. [[CrossRef](#)] [[PubMed](#)]
46. Huang, D.W.; Sherman, B.T.; Lempicki, R.A. Systematic and integrative analysis of large gene lists using DAVID bioinformatics resources. *Nat. Protoc.* **2009**, *4*, 44–57. [[CrossRef](#)]
47. Eden, E.; Navon, R.; Steinfeld, I.; Lipson, D.; Yakhini, Z. GOrilla: A tool for discovery and visualization of enriched GO terms in ranked gene lists. *BMC Bioinform.* **2009**, *10*, 48. [[CrossRef](#)]
48. Kumpost, J.; Syrova, Z.; Kulihova, L.; Frankova, D.; Bologna, J.-C.; Hlavackova, V.; Prezeau, L.; Kralikova, M.; Hruskova, B.; Pin, J.-P.; et al. Surface expression of metabotropic glutamate receptor variants mGluR1a and mGluR1b in transfected HEK293 cells. *Neuropharmacology* **2008**, *55*, 409–418. [[CrossRef](#)]
49. Techlovská, Š.; Chambers, J.N.; Dvořáková, M.; Petralia, R.S.; Wang, Y.-X.; Hájková, A.; Nová, A.; Franková, D.; Prezeau, L.; Blahos, J. Metabotropic glutamate receptor 1 splice variants mGluR1a and mGluR1b combine in mGluR1a/b dimers in vivo. *Neuropharmacology* **2014**, *86*, 329–336. [[CrossRef](#)]
50. Naito, R.; Kassai, H.; Sakai, Y.; Schönherr, S.; Fukaya, M.; Schwarzer, C.; Sakagami, H.; Nakao, K.; Aiba, A.; Ferraguti, F. New Features on the Expression and Trafficking of mGluR1 Splice Variants Exposed by Two Novel Mutant Mouse Lines. *Front. Mol. Neurosci.* **2018**, *11*, 439. [[CrossRef](#)]
51. Ohtani, Y.; Miyata, M.; Hashimoto, K.; Tabata, T.; Kishimoto, Y.; Fukaya, M.; Kase, D.; Kassai, H.; Nakao, K.; Hirata, T.; et al. The synaptic targeting of mGluR1 by its carboxyl-terminal domain is crucial for cerebellar function. *J. Neurosci.* **2014**, *34*, 2702–2712. [[CrossRef](#)]
52. Mundell, S.J.; Matharu, A.-L.; Pula, G.; Holman, D.; Roberts, P.J.; Kelly, E. Metabotropic Glutamate Receptor 1 Internalization Induced by Muscarinic Acetylcholine Receptor Activation: Differential Dependency of Internalization of Splice Variants on Nonvisual Arrestins. *Mol. Pharmacol.* **2002**, *61*, 1114–1123. [[CrossRef](#)]
53. Ady, V.; Perroy, J.; Tricoire, L.; Piochon, C.; Dadak, S.; Chen, X.; Dusart, I.; Fagni, L.; Lambolez, B.; Levenes, C. Type 1 metabotropic glutamate receptors (mGlu1) trigger the gating of GluD2 delta glutamate receptors. *EMBO Rep.* **2014**, *15*, 103–109. [[CrossRef](#)]
54. Kitano, J.; Nishida, M.; Itsukaichi, Y.; Minami, I.; Ogawa, M.; Hirano, T.; Mori, Y.; Nakanishi, S. Direct interaction and functional coupling between metabotropic glutamate receptor subtype 1 and voltage-sensitive Cav2.1 Ca²⁺ channel. *J. Biol. Chem.* **2003**, *278*, 25101–25108. [[CrossRef](#)]
55. Werthmann, R.C.; Tzouros, M.; Lamerz, J.; Augustin, A.; Fritzius, T.; Trovò, L.; Stawarski, M.; Raveh, A.; Diener, C.; Fischer, C.; et al. Symmetric signal transduction and negative allosteric modulation of heterodimeric mGlu1/5 receptors. *Neuropharmacology* **2021**, *190*, 108426. [[CrossRef](#)]
56. Doumazane, E.; Scholler, P.; Zwier, J.M.; Trinquet, E.; Rondard, P.; Pin, J. A new approach to analyze cell surface protein complexes reveals specific heterodimeric metabotropic glutamate receptors. *FASEB J.* **2011**, *25*, 66–77. [[CrossRef](#)]
57. Hanson, J.E.; Smith, Y. Group I metabotropic glutamate receptors at GABAergic synapses in monkeys. *J. Neurosci.* **1999**, *19*, 6488–6496. [[CrossRef](#)]
58. Mansouri, M.; Kasugai, Y.; Fukazawa, Y.; Bertaso, F.; Raynaud, F.; Perroy, J.; Fagni, L.; Kaufmann, W.A.; Watanabe, M.; Shigemoto, R.; et al. Distinct subsynaptic localization of type 1 metabotropic glutamate receptors at glutamatergic and GABAergic synapses in the rodent cerebellar cortex. *Eur. J. Neurosci.* **2015**, *41*, 157–167. [[CrossRef](#)]
59. Gassmann, M.; Bettler, B. Regulation of neuronal GABA_B receptor functions by subunit composition. *Nat. Rev. Neurosci.* **2012**, *13*, 380–394. [[CrossRef](#)]
60. Zheng, S.; Abreu, N.; Levitz, J.; Kruse, A.C. Structural basis for KCTD-mediated rapid desensitization of GABA_B signalling. *Nature* **2019**, *567*, 127–131. [[CrossRef](#)]
61. Zuo, H.; Glaaser, I.; Zhao, Y.; Kurinov, I.; Mosyak, L.; Wang, H.; Liu, J.; Park, J.; Frangaj, A.; Sturchler, E.; et al. Structural basis for auxiliary subunit KCTD16 regulation of the GABA_B receptor. *Proc. Natl. Acad. Sci. USA* **2019**, *116*, 8370–8379. [[CrossRef](#)]
62. Schwenk, J.; Metz, M.; Zolles, G.; Turecek, R.; Fritzius, T.; Bildl, W.; Tarusawa, E.; Kulik, A.; Unger, A.; Ivankova, K.; et al. Native GABA_B receptors are heteromultimers with a family of auxiliary subunits. *Nature* **2010**, *465*, 231–235. [[CrossRef](#)] [[PubMed](#)]
63. Yamasaki, M.; Aiba, A.; Kano, M.; Watanabe, M. mGluR1 signaling in cerebellar Purkinje cells: Subcellular organization and involvement in cerebellar function and disease. *Neuropharmacology* **2021**, *194*, 108629. [[CrossRef](#)] [[PubMed](#)]
64. Ferraguti, F.; Baldani-Guerra, B.; Corsi, M.; Nakanishi, S.; Corti, C. Activation of the extracellular signal-regulated kinase 2 by metabotropic glutamate receptors. *Eur. J. Neurosci.* **1999**, *11*, 2073–2082. [[CrossRef](#)] [[PubMed](#)]
65. Turecek, R.; Schwenk, J.; Fritzius, T.; Ivankova, K.; Zolles, G.; Adelfinger, L.; Jacquier, V.; Besseyrias, V.; Gassmann, M.; Schulte, U.; et al. Auxiliary GABA_B receptor subunits uncouple G protein βγ subunits from effector channels to induce desensitization. *Neuron* **2014**, *82*, 1032–1044. [[CrossRef](#)] [[PubMed](#)]
66. Baude, A.; Nusser, Z.; Roberts, J.D.; Mulvihill, E.; McIlhinney, R.A.; Somogyi, P. The metabotropic glutamate receptor (mGluR1 alpha) is concentrated at perisynaptic membrane of neuronal subpopulations as detected by immunogold reaction. *Neuron* **1993**, *11*, 771–787. [[CrossRef](#)] [[PubMed](#)]
67. Kulik, A.; Nakadate, K.; Nyíri, G.; Notomi, T.; Malitschek, B.; Bettler, B.; Shigemoto, R. Distinct localization of GABA_B receptors relative to synaptic sites in the rat cerebellum and ventrobasal thalamus. *Eur. J. Neurosci.* **2002**, *15*, 291–307. [[CrossRef](#)]
68. Mao, L.-M.; Bodepudi, A.; Chu, X.-P.; Wang, J.Q. Group I Metabotropic Glutamate Receptors and Interacting Partners: An Update. *Int. J. Mol. Sci.* **2022**, *23*, 840. [[CrossRef](#)]

69. Mundell, S.J.; Pula, G.; McIlhinney, R.A.J.; Roberts, P.J.; Kelly, E. Desensitization and internalization of metabotropic glutamate receptor 1a following activation of heterologous Gq/11-coupled receptors. *Biochemistry* **2004**, *43*, 7541–7551. [[CrossRef](#)]
70. Jin, D.-Z.; Guo, M.-L.; Xue, B.; Fibuch, E.E.; Choe, E.S.; Mao, L.-M.; Wang, J.Q. Phosphorylation and feedback regulation of metabotropic glutamate receptor 1 by calcium/calmodulin-dependent protein kinase II. *J. Neurosci.* **2013**, *33*, 3402–3412. [[CrossRef](#)]
71. van Woerden, G.M.; Hoebeek, F.E.; Gao, Z.; Nagaraja, R.Y.; Hoogenraad, C.C.; Kushner, S.A.; Hansel, C.; De Zeeuw, C.I.; Elgersma, Y. betaCaMKII controls the direction of plasticity at parallel fiber-Purkinje cell synapses. *Nat. Neurosci.* **2009**, *12*, 823–825. [[CrossRef](#)]
72. Zhang, J.; Zhou, Y. 14-3-3 Proteins in Glutamatergic Synapses. *Neural Plast.* **2018**, *2018*, 8407609. [[CrossRef](#)]
73. Abramow-Newerly, M.; Roy, A.A.; Nunn, C.; Chidiac, P. RGS proteins have a signalling complex: Interactions between RGS proteins and GPCRs, effectors, and auxiliary proteins. *Cell. Signal.* **2006**, *18*, 579–591. [[CrossRef](#)]
74. Gabriel, L.; Lvov, A.; Orthodoxou, D.; Rittenhouse, A.R.; Kobertz, W.R.; Melikian, H.E. The acid-sensitive, anesthetic-activated potassium leak channel, KCNK3, is regulated by 14-3-3 β -dependent, protein kinase C (PKC)-mediated endocytic trafficking. *J. Biol. Chem.* **2012**, *287*, 32354–32366. [[CrossRef](#)]
75. Pandya, N.J.; Klaassen, R.V.; van der Schors, R.C.; Slotman, J.A.; Houtsmuller, A.; Smit, A.B.; Li, K.W. Group 1 metabotropic glutamate receptors 1 and 5 form a protein complex in mouse hippocampus and cortex. *Proteomics* **2016**, *16*, 2698–2705. [[CrossRef](#)]
76. Shrivastava, A.N.; Triller, A.; Melki, R. Cell biology and dynamics of Neuronal Na⁺/K⁺-ATPase in health and diseases. *Neuropharmacology* **2020**, *169*, 107461. [[CrossRef](#)]
77. Aittaleb, M.; Boguth, C.A.; Tesmer, J.J.G. Structure and function of heterotrimeric G protein-regulated Rho guanine nucleotide exchange factors. *Mol. Pharmacol.* **2010**, *77*, 111–125. [[CrossRef](#)]
78. Ba, W.; Nadif Kasri, N. RhoGTPases at the synapse: An embarrassment of choice. *Small GTPases* **2017**, *8*, 106–113. [[CrossRef](#)]
79. Hirono, M.; Yoshioka, T.; Konishi, S. GABA(B) receptor activation enhances mGluR-mediated responses at cerebellar excitatory synapses. *Nat. Neurosci.* **2001**, *4*, 1207–1216. [[CrossRef](#)]
80. Tabata, T.; Araishi, K.; Hashimoto, K.; Hashimotodani, Y.; van der Putten, H.; Bettler, B.; Kano, M. Ca²⁺ activity at GABA B receptors constitutively promotes metabotropic glutamate signaling in the absence of GABA. *Proc. Natl. Acad. Sci. USA* **2004**, *101*, 16952–16957. [[CrossRef](#)]
81. Kamikubo, Y.; Tabata, T.; Kakizawa, S.; Kawakami, D.; Watanabe, M.; Ogura, A.; Iino, M.; Kano, M. Postsynaptic GABA_B receptor signalling enhances LTD in mouse cerebellar Purkinje cells. *J. Physiol.* **2007**, *585*, 549–563. [[CrossRef](#)]
82. Rives, M.-L.; Vol, C.; Fukazawa, Y.; Tinel, N.; Trinquet, E.; Ayoub, M.A.; Shigemoto, R.; Pin, J.-P.; Prézeau, L. Crosstalk between GABA_B and mGlu1a receptors reveals new insight into GPCR signal integration. *EMBO J.* **2009**, *28*, 2195–2208. [[CrossRef](#)] [[PubMed](#)]
83. Hildebrand, M.E.; Isope, P.; Miyazaki, T.; Nakaya, T.; Garcia, E.; Feltz, A.; Schneider, T.; Hescheler, J.; Kano, M.; Sakimura, K.; et al. Functional Coupling between mGluR1 and Cav3.1 T-Type Calcium Channels Contributes to Parallel Fiber-Induced Fast Calcium Signaling within Purkinje Cell Dendritic Spines. *J. Neurosci.* **2009**, *29*, 9668–9682. [[CrossRef](#)] [[PubMed](#)]
84. Canepari, M.; Ogden, D. Kinetic, pharmacological and activity-dependent separation of two Ca²⁺ signalling pathways mediated by type 1 metabotropic glutamate receptors in rat Purkinje neurones. *J. Physiol.* **2006**, *573*, 65–82. [[CrossRef](#)] [[PubMed](#)]
85. Netzeband, J.G.; Gruol, D.L. mGluR1 agonists elicit a Ca²⁺ signal and membrane hyperpolarization mediated by apamin-sensitive potassium channels in immature rat purkinje neurons. *J. Neurosci. Res.* **2008**, *86*, 293–305. [[CrossRef](#)]
86. Bhandari, P.; Vandael, D.; Fernández-Fernández, D.; Fritzius, T.; Kleindienst, D.; Önal, C.; Montanaro, J.; Gassmann, M.; Jonas, P.; Kulik, A.; et al. GABA_B receptor auxiliary subunits modulate Cav2.3-mediated release from medial habenula terminals. *Elife* **2021**, *10*, e68274. [[CrossRef](#)]

Disclaimer/Publisher’s Note: The statements, opinions and data contained in all publications are solely those of the individual author(s) and contributor(s) and not of MDPI and/or the editor(s). MDPI and/or the editor(s) disclaim responsibility for any injury to people or property resulting from any ideas, methods, instructions or products referred to in the content.